Chapter 4

Effective Properties of Short-fiber Piezoelectric Composites

4.1 Introduction

Recently, piezoelectric materials have gained a huge attention in the field of smart materials due to their sensing and actuating capabilities. These materials have an excellent property of converting energy from a mechanical to an electrical domain and vice-versa. This property of reciprocity in the energy conversions makes them a wonderful class of materials to have many advanced applications, e.g., structural health monitoring, vibration and noise control, ultrasonic imaging, aeroelastic control, underwater applications and numerous such applications. However, bulk use of monolithic materials has several drawbacks hence composite materials of tailored properties could be fabricated to attain better technological solutions to many such limitations.

In order to design such composites many analytical models have been presented in the literature. Most of these techniques that have been developed to predict the effective electromechanical coefficients depend upon the solution provided by Eshelby's ellipsoidal inclusion model embedded in an infinite medium. The self-consistent scheme, differential scheme, Mori-Tanaka approximation, dilute scheme, the asymptotic homogenization method [23,27,28,31,32] are few such analytical techniques. All of these techniques are based on assumptions of constant stress and strains in the inclusion under uniform load and a far field of electrical load and traction is applied on the boundary. Hence, local field fluctuations are not effectively captured in these studies. The local field fluctuations can be better modelled in finite element method by deducing whole macroscopic composite into smaller units viz. unit cell approach. These representative

volume elements (RVE) are chosen by repeating these units in three dimensional structures to give the bulk of material. Any study regarding effective property on such RVE will yield results for the bulk material when a volume averaging of results are done. Based on the FEM based approach many studies have been carried out to evaluate the effective properties of piezoelectric composites, such studies primarily contain the problems associated with composites having long fibers either as circular cylinder or square column embedded in the matrix phases [121–123].

However, studies regarding piezoelectric composite containing short fibers are rare and negligible in literature. Bohm and Segurado [124,125] have calculated the effective coefficients of piezoelectric composites containing randomly distributed spherical particles using random sequential adsorption (RSA) algorithm. In [126,127], Hine *et. al.* have conducted the experiments to evaluate the effective properties of randomly distributed short fiber composites and the results have been compared with numerical results. Kari *et. al.* [128] have studied the influence of the size of spherical filler particles and of the RVE on the effective material properties of piezoelectric particulate composite with FEM approach. A numerical model based on fixed grid finite elements has been developed by Bao *et. al.* [129] to present an approximation of effective moduli of particulate composite. The model effectively helps avoid the difficulty of domain discretization caused by the inclusion with the conventional FEM approach. In [129], Bao *et. al.* have evaluated the effective properties of piezoelectric particulate composites numerically with a FEM based model. The finite element model developed in this work is based on the generalization of simplified strain gradient and distortion gradient elasticity theories. The model effectively predicts the strong positive side effects for the composites with smaller inclusions as compared with material length scale parameters. But, because of the limited amount of the work which deals with predicting effective

coefficients of piezoelectric particulate composites we have been motivated to work in this direction.

In this chapter an attempt is made to generate higher volume fraction RVE models with different size and packing arrangements of piezoelectric inclusion in matrix medium. The effective electro-elastic properties are estimated using numerical homogenization techniques (using FEM approach) and periodic boundary conditions. The solution of Eshelby's inclusion problem has been modified for this problem in order to get effective properties of short fiber composite containing spheroidal inclusion (fiber). The numerical results have been derived through finite element analysis based on the unit cell approach of two possible fiber arrangements, i.e., simple cubic (SC) and body centred cubic (BCC). A comparative study has been presented for both these methods, i.e., analytical method based on Eshelby's solution and numerical method based on finite element approach.

4.2 Coupled Electro-Elastic Fields Modeling inside an Inclusion

In an infinite medium D, the domain of a piezoelectric inclusion can be mathematically given as

$$\Omega: \frac{x_1^2}{a_1^2} + \frac{x_2^2}{a_2^2} + \frac{x_3^2}{a_3^2} \leq 1 \tag{4.1}$$

where a_1, a_2 and $a_3$are the lengths of the semi axes of the ellipsoid. The surface area of the inclusion is denoted by IΩI ,and the entire domain by *D*. First considering inclusion has the same electroelastic moduli as that of matrix, but is allowed to undergo a uniform stress-free strain ε_{mn}^*, and electric displacement-free electric field, E_n^* represented by Z_{Mn}^*. To calculate the stress, strain, electric displacement, and electric field, a generalization of the imaginary cutting, straining, and welding operations used by [23] are utilized.

Adopting a shorthand notation introduced by [119], electroeleastic constants can be expressed on equal footing in the following as

$$L_{iJMn} = \begin{cases} C_{ijmn} & J, M = 1,2,3 \\ e_{nij} & J = 1,2,3; M = 4 \\ e_{imn} & J = 4; M = 1,2,3 \\ -\kappa_{in} & J, M = 4 \end{cases} \tag{4.2}$$

Assuming the same shorthand format, the combined coupled electroeleastic field can be unified into a single equation

$$\Sigma_{iJ} = L_{iJMn} Z_{Mn} \tag{4.3}$$

where

$$\Sigma_{iJ} = \begin{cases} \sigma_{ij} & J = 1,2,3 \\ D_i & J = 4 \end{cases}, \tag{4.4a}$$

and

$$Z_{Mn} = \begin{cases} \varepsilon_{mn} & M = 1,2,3 \\ -E_n & M = 4 \end{cases}. \tag{4.4b}$$

In the above equations σ_{ij} is elastic stress, D_i electric displacement vector, ε_{mn} elastic strain, E_n electric field. Lowercase Latin subscripts range from 1 to 3, while uppercase subscripts range from 1 to 4.

$$U_M = \begin{cases} u_m & M = 1,2,3 \\ \phi & M = 4 \end{cases} \tag{4.5}$$

where u_m is elastic displacement, and ϕ is electric potential.

Equilibrium Conditions:

Since eigenfields are present for inclusion only and absent in rest of the domain the stress and electric displacement can be expressed by the linear piezoelectric constitutive equation

$$\Sigma_{iJ}(x) = L_{iJMn}\left(U_{M,n} - Z^{*}_{Mn}\right) \tag{4.6}$$

In the absence of any external excitation the electroelastic equilibrium condition is expressed as

$$\Sigma_{iJ,i} = 0 \tag{4.7}$$

Substitution of Eqn. (4.7) into Eqn. (4.6) leads to

$$L_{iJMn}U_{M,ni} = L_{iJMn}Z^{*}_{Mn,i} \tag{4.8}$$

It can be clearly noticed from Eqn. (4.8) that $L_{iJMn}Z^{*}_{Mn,i}$ behaves like a body force and electric charge in the piezoelectric material. The solution to the fundamental Eqn. (4.8) will give $U_M(x)$.

The linear theory of elasticity allows for the superposition of solutions. Applying, Fourier series form the solution to Eqn. (4.8) can be derived as

$$Z^{*}_{Mn}(x) = \sum \bar{Z}^{*}_{Mn}(\xi) exp(i\xi.x) \tag{4.9}$$

Putting Eqn. (4.9) in Eqn. (4.8) and solving for $U_M(x)$ we get

$$U_M(x) = -i(2\pi)^{-3}\int_{-\infty}^{\infty}\int_{-\infty}^{\infty} L_{iJMn}Z^{*}_{Mn}(x')\xi_l N_{MJ}(\xi)D^{-1}(\xi)exp\{i\xi.(x - x')\}d\xi dx' \tag{4.10}$$

or,

$$U_M(x) = -L_{iJAb}\int_{-\infty}^{\infty} Z^{*}_{Ab}(x')G_{MJ,i}(x - x')dx' \tag{4.11}$$

where

$$G_{MJ}(x - x') = -2\pi^{-3}\int_{-\infty}^{\infty} N_{MJ}(\xi)D^{-1}(\xi)exp\left(i\xi.(x - x')\right)d\xi \tag{4.12}$$

is Green's function. It is defined as displacement component in x_m –direction at point x when a unit body force in the x_j –direction is applied at point x' in the infinitely extended material.

In Eqn. (4.12) $N_{MJ}(\xi)$ and $D(\xi)$ being the cofactors and the determinant of the 4×4 matrix $L_{iMJn}\xi_i\xi_n$, respectively. It is noted that $N_{MJ}(\xi) = N_{JM}(\xi)$ owing to symmetry of the electroelastic constants L_{iMJn}.

Eqn. (4.10) can be reduced in simple form assuming eigenfields Z^*_{Mn} are uniformly distributed in the ellipsoidal inclusion and using these transformations

$$x_1/a_1 = y_1\,,\ x_2/a_2 = y_2\,,\ x_3/a_3 = y_3$$

$$a_1\bar{\xi}_1 = \zeta_1,\quad a_2\bar{\xi}_2 = \zeta_2,\quad a_3\bar{\xi}_3 = \zeta_3,$$

$$\zeta_1/\zeta = \bar{\zeta}_1,\quad \zeta_2/\zeta = \bar{\zeta}_2,\quad \zeta_3/\zeta = \bar{\zeta}_3,$$

$$\zeta = (\zeta_1^2 + \zeta_1^2 + \zeta_3^2)^{1/2},$$

$$dS(\bar{\zeta}) = a_1a_2a_3\zeta^{-3}dS(\bar{\zeta}) \tag{4.13}$$

With the above transformations, the induced elastic displacement and electric potential within the inclusion becomes

$$U_M(x - x') = \frac{1}{4\pi}L_{iJAb}Z^*_{Ab}\bar{G}_{MJin}x_n \tag{4.14}$$

Equation (4.14) is similar to that of [27] for the elastic inclusion problem. Combining Eqns. (4.4a-b) and (4.14), the induced strain and electric fields due to the uniform eigenfields in the inclusion are given by

$$Z_{Mn} = S_{MnAb} Z^*_{Ab} \tag{4.15}$$

where

$$S_{MnAb} = \begin{cases} \frac{1}{8\pi} L_{iJAb}\left(\bar{G}_{mJin} + \bar{G}_{nJim}\right) & M = 1,2,3 \\ \frac{1}{4\pi} L_{iJAb} \bar{G}_{4Jin} & M = 4 \end{cases} \tag{4.16}$$

are referred to as Eshelby tensors for anisotropic piezoelectric materials.

The corresponding stress σ_{ij} and electric displacement D_i inside the inclusion due to a uniform eigenfield in Ω can be derived from the constitutive equation for a piezoelectric material given by [31]

$$\sigma_{ij} = C_{ijmn}(S_{mnab}\varepsilon^*_{ab} - S_{mn4b}E^*_b - \varepsilon^*_{mn}) - e_{nij}(S_{4n4b}E^*_b - S_{4nab}\varepsilon^*_{ab} - E^*_n)\,, \tag{4.17a}$$

$$D_i = e_{imn}(S_{mnab}\varepsilon^*_{ab} - S_{mn4b}E^*_b - \varepsilon^*_{mn}) + \kappa_{in}(S_{4n4b}E^*_b - S_{4nab}\varepsilon^*_{ab} - E^*_n)\,. \tag{4.17b}$$

Both the piezoelectric matrix and the inclusion are considered to be transversely isotropic *(6mm symmetry)* and for simplicity, the crystalline direction of the matrix is assumed to be coincident with the principal axis of the inclusion. Adopting Voigt two-index notation, elastic, piezoelectric and dielectric constants L_{iMJn} transfers to a 9 × 9 matrix as follows:

$$\left[L_{iJMn}\right] = \begin{bmatrix} C_{11} & C_{12} & C_{13} & 0 & 0 & 0 & 0 & 0 & -e_{31} \\ C_{12} & C_{11} & C_{13} & 0 & 0 & 0 & 0 & 0 & -e_{31} \\ C_{13} & C_{12} & C_{33} & 0 & 0 & 0 & 0 & 0 & -e_{33} \\ 0 & 0 & 0 & C_{44} & 0 & 0 & 0 & -e_{15} & 0 \\ 0 & 0 & 0 & 0 & C_{44} & 0 & -e_{15} & 0 & 0 \\ 0 & 0 & 0 & 0 & 0 & C_{66} & 0 & 0 & 0 \\ 0 & 0 & 0 & 0 & e_{15} & 0 & \kappa_{11} & 0 & 0 \\ 0 & 0 & 0 & e_{15} & 0 & 0 & 0 & \kappa_{11} & 0 \\ e_{31} & e_{31} & e_{33} & 0 & 0 & 0 & 0 & 0 & \kappa_{33} \end{bmatrix} \tag{4.18}$$

In this case Eqns. 4.17(a)-(b) and 4.18 takes the form

$$\varepsilon_{mn} = S_{mnab}\varepsilon^*_{ab} - S_{mn4b}E^*_b \tag{4.19a}$$

$$E_n = S_{4n4b}E^*_b - S_{4nab}\varepsilon^*_{ab} \tag{4.19b}$$

where

$$S_{mnab} = \frac{1}{8\pi}\left[C_{ijab}\left(\bar{G}_{mjin} + \bar{G}_{njim}\right) - e_{iab}(\bar{G}_{m4in} + \bar{G}_{n4im})\right],$$

$$S_{mn4b} = \frac{1}{8\pi}\left[e_{bij}\left(\bar{G}_{mjin} + \bar{G}_{njim}\right) + \kappa_{ib}(\bar{G}_{m4in} + \bar{G}_{n4im})\right]$$

$$S_{4nab} = \frac{1}{4\pi}\left(C_{ijab}\bar{G}_{4jin} - e_{iab}\bar{G}_{44in}\right)$$

$$S_{4n4b} = \frac{1}{4\pi}\left(e_{bij}\bar{G}_{4jin} + \kappa_{ib}\bar{G}_{44in}\right) \tag{4.20}$$

4.3 Calculation of Effective Properties

For a sufficiently large two-phase composite D consists of randomly oriented multiple inhomogeneities Ω (=Ω_1+ $\Omega_{2+\ldots\ldots+}$ Ω_N) with electro-elastic constants L^*_{iJMn} and the volume fraction *f*. The surrounding matrix is denoted by D-Ω and has electro-elastic constants L_{iJMn}. Here $L_{iJMn} = L^*_{iJMn} = 0$ for a piezoelectric material when one subscript is 4. To determine the effective elastic, piezoelectric, dielectric constants of the composite, the Mori-Tanaka mean-field theory is employed.

Considering this theory, piezoelectric composite be subjected to the far-field traction, electric displacement $\Sigma^0_{ij}n_i$ on the boundary with outward unit normal vector n_i and in the absence of the inhomogeneities Ω, the strain and electric field Z^0_{Mn} distributes uniformly. Now, the presence of a random inhomogeneity Ω_k creates disturbance in local fields of both matrix and the *k*th inhomogeneity. Since the volume average of the disturbance portion of the stress, electric displacement vanishes it can be written as

$$\int \Sigma_{iJ}\, dx = 0, \tag{4.21}$$

and in addition,

$$(1-f)\langle \Sigma_{ij}^{m} \rangle + f\langle \Sigma_{ij}^{\Omega} \rangle = 0. \tag{4.22}$$

The average disturbed stress, electric displacement in the matrix and the kth inhomogeneity can respectively be written as

$$\langle \Sigma_{ij}^{m} \rangle = L_{iJMn}\langle \mathrm{Z}_{Mn}^{m} \rangle \quad \text{in } D-\Omega \tag{4.23}$$

$$\langle \Sigma_{ij}^{\Omega_k} \rangle = L_{iJMn}^{*}(\langle \mathrm{Z}_{Mn}^{m} \rangle + \langle Z_{Mn} \rangle) \text{ in } \Omega_k, \tag{4.24}$$

where $\langle \mathrm{Z}_{Mn}^{m} \rangle$ are the average strain, electric fields in the matrix, $\langle Z_{Mn} \rangle$ the average disturbance of the otherwise uniform strain, electric fields in Ω_k. Since all the inhomogeneities are of the same shape with the same material properties, the average value over Ω_k is identical with that over Ω, namely $\langle \Sigma_{ij}^{\Omega_k} \rangle = \langle \Sigma_{ij}^{\Omega} \rangle$.

When the piezoelectric composite is subjected to the uniform far-field mechanical load, electric displacement Σ_{ij}^{0}, the following effect due to this excitation can be mathematically expressed as

$$\Sigma_{ij}^{0} + \langle \Sigma_{ij}^{\Omega} \rangle = L_{iJMn}^{*}(\mathrm{Z}_{Mn}^{0} + \langle \mathrm{Z}_{Mn}^{m} \rangle + Z_{Mn}). \tag{4.25}$$

Since the applied electromechanical load is uniform through the inhomogeneity $\langle Z_{Mn} \rangle = Z_{Mn}$ in Ω has been used in the above equation.

Considering the equivalent inclusion method [23], Eqn. (4.25) can be written as

$$\begin{aligned} \Sigma_{ij}^{0} + \langle \Sigma_{ij}^{\Omega} \rangle &= L_{iJMn}^{*}(\mathrm{Z}_{Mn}^{0} + \langle \mathrm{Z}_{Mn}^{m} \rangle + Z_{Mn}) \\ &= L_{iJMn}^{*}(\mathrm{Z}_{Mn}^{0} + \langle \mathrm{Z}_{Mn}^{m} \rangle + Z_{Mn} - \mathrm{Z}_{Mn}^{*}) \end{aligned} \tag{4.26}$$

In above equation disturbed field Z_{Mn} can be related to the fictitious eigenfield Z_{Mn}^{*} by

$$Z_{Mn} = S_{MnAb}\mathrm{Z}^{*}_{Ab}. \tag{4.27}$$

The average disturbance of stress, electric displacement in the inhomogeneity can be written by substituting Eqn. (4.26) into Eqn. (4.25) as

$$\langle \Sigma^{\Omega}_{ij} \rangle = L_{iJMn}\langle \mathrm{Z}^{m}_{Mn} \rangle + L_{iJMn}(S_{MnAb} - I_{MnAb})\mathrm{Z}^{*}_{Ab}\,, \tag{4.28}$$

Combining Eqns. (4.22), (4.24), and (4.28) leads to

$$\langle \mathrm{Z}^{m}_{Mn} \rangle = -f(S_{MnAb} - I_{MnAb})\mathrm{Z}^{*}_{Ab}\,. \tag{4.29}$$

Substitution of Eq. (4.27) into Eqns. (4.23) and (4.27), respectively, then yields

$$\langle \Sigma^{m}_{ij} \rangle = -fL_{iJMn}(S_{MnAb} - I_{MnAb})\mathrm{Z}^{*}_{Ab}\,, \tag{4.30}$$

$$\langle \Sigma^{\Omega}_{ij} \rangle = (1-f)L_{iJMn}(S_{MnAb} - I_{MnAb})\mathrm{Z}^{*}_{Ab}. \tag{4.31}$$

The equivalent eigenstrain, eigenelectric field Z^{*}_{Ab} are solved by substituting Eqn. (4.28) into the equivalent Eqn. (4.26). Thus, we have

$$\mathrm{Z}^{*}_{Ab} = U^{-1}_{AbiJ}(L^{*}_{iJMn} - L_{iJMn})\mathrm{Z}^{0}_{Mn}\,, \tag{4.32}$$

where

$$U_{iJAb} = \left(L^{*}_{iJMn} - L_{iJMn}\right)[(1-f)S_{MnAb} + fI_{MnAb}] + L_{iJAb}. \tag{4.33}$$

The weighted average of that over each phase will give overall strain, electric fields, $\langle \mathrm{Z}^{c}_{Mn} \rangle$, written below

$$\langle \mathrm{Z}^{c}_{Mn} \rangle = \frac{1}{V}\left(\int (\mathrm{Z}^{0}_{Mn} + \langle \mathrm{Z}^{m}_{Mn} \rangle)d\boldsymbol{x} + \int (\mathrm{Z}^{0}_{Mn} + \langle \mathrm{Z}^{\Omega}_{Mn} \rangle)d\boldsymbol{x}\right). \tag{4.34}$$

where V denoted the volume of the entire composite. Substituting Eqns. (4.27) and (4.29) into the equation above yields

$$\langle \mathrm{Z}^{c}_{Mn} \rangle = \mathrm{Z}^{0}_{Mn} + f\mathrm{Z}^{*}_{Mn}. \tag{4.35}$$

Following the equivalent eigen fields Z^{*}_{Mn} shown by Eqn. (4.32), the overall strain, electric field $\langle \mathrm{Z}^{c}_{Mn} \rangle$ can be written as

$$\langle \mathrm{Z}^{c}_{Mn} \rangle = \overline{L^{-1}_{Mn\imath J}} \Sigma^{0}_{iJ} \,, \tag{4.36}$$

where $\overline{L^{-1}_{Mn\imath J}}$ is the effective electroelastic compliance of the composite. Mathematically expressed as

$$\overline{L^{-1}_{Mn\imath J}} = [I_{MnAb} - f U^{-1}_{MnqR}(L^{*}_{qRAb} - L_{qRAb}) L^{-1}_{AbiJ} \tag{4.37}$$

Following the same procedure, the effective electroelastic moduli $\overline{L_{\imath JMn}}$ can be derived as

$$\overline{L_{\imath JMn}} = L_{iJAb}\left[I_{AbMn} + f V^{-1}_{AbqR}\left(L^{*}_{qRMn} - L_{qRMn}\right)\right] , \tag{4.38}$$

where

$$V_{iJAb} = (1-f)\left(L^{*}_{iJMn} - L_{iJMn}\right) S_{MnAb} + L_{iJAb} \,. \tag{4.39}$$

It can be shown that the effective electroelastic stiffness $\overline{L_{\imath JMn}}$ given by Eqn. (4.39) and compliance $\overline{L^{-1}_{Mn\imath J}}$ given by Eqn. (4.38) are reciprocal to each other, namely $\overline{L^{-1}_{Mn\imath J}} L_{iJAb} = I_{MnAb}$.

4.4 Finite Element Modeling

The linear constitutive behaviour of piezoelectric material can be mathematically expressed as

$$T_{ij} = C^{E}_{ijkl} S_{kl} - e_{kij} E_{k} \tag{4.40a}$$

$$D_{i} = e_{ikl} S_{kl} + \kappa^{\epsilon}_{ik} E_{k} \tag{4.40b}$$

where σ_{ij}, ϵ_{kl}, E_k, D_i in above equation represents the stress, strain, electric field and electric displacement tensors respectively and C_{ijkl}^{E}, κ_{ik}^{ϵ}, e_{ikl} represents elastic constants, dielectric constants, piezoelectric constant tensor respectively for the materials.

The problem in this chapter has been dealt with assuming that the piezoelectric materials are poled along x_3 direction (x_1, x_2 as isotropic plane). So, in matrix form the above equation can be written with 10 independent coefficients as

$$\begin{Bmatrix} \langle T_{11} \rangle \\ \langle T_{22} \rangle \\ \langle T_{33} \rangle \\ \langle T_{23} \rangle \\ \langle T_{31} \rangle \\ \langle T_{12} \rangle \\ \langle D_1 \rangle \\ \langle D_2 \rangle \\ \langle D_3 \rangle \end{Bmatrix} = \begin{bmatrix} C_{11}^{eff} & C_{12}^{eff} & C_{13}^{eff} & 0 & 0 & 0 & 0 & 0 & -e_{31}^{eff} \\ C_{12}^{eff} & C_{11}^{eff} & C_{13}^{eff} & 0 & 0 & 0 & 0 & 0 & -e_{31}^{eff} \\ C_{13}^{eff} & C_{13}^{eff} & C_{33}^{eff} & 0 & 0 & 0 & 0 & 0 & -e_{33}^{eff} \\ 0 & 0 & 0 & C_{44}^{eff} & 0 & 0 & 0 & -e_{15}^{eff} & 0 \\ 0 & 0 & 0 & 0 & C_{44}^{eff} & 0 & -e_{15}^{eff} & 0 & 0 \\ 0 & 0 & 0 & 0 & 0 & C_{66}^{eff} & 0 & 0 & 0 \\ 0 & 0 & 0 & 0 & e_{15}^{eff} & 0 & \kappa_{11}^{eff} & 0 & 0 \\ 0 & 0 & 0 & e_{15}^{eff} & 0 & 0 & 0 & \kappa_{11}^{eff} & 0 \\ e_{31}^{eff} & e_{31}^{eff} & e_{33}^{eff} & 0 & 0 & 0 & 0 & 0 & \kappa_{33}^{eff} \end{bmatrix} \begin{Bmatrix} \langle S_{11} \rangle \\ \langle S_{22} \rangle \\ \langle S_{33} \rangle \\ \langle S_{23} \rangle \\ \langle S_{31} \rangle \\ \langle S_{12} \rangle \\ \langle E_1 \rangle \\ \langle E_2 \rangle \\ \langle E_3 \rangle \end{Bmatrix} \tag{4.41}$$

The overall behaviour of the piezoelectric composite can be predicted by determining effective elastic constants C_{ijkl}^{eff}, effective piezoelectric constants e_{ikl}^{eff} and effective dielectric constants κ_{ik}^{eff}. $\langle \dots \rangle$ denotes the spatial average value for directional stresses and strains. These overall effective properties depend primarily upon material properties of fiber and matrix phases and fiber orientation and geometries. Since the fiber geometries

can vary from being ellipsoidal, cylindrical to spherical (in case of composites containing short fibers), in present study spheroidal shape fiber of two possible arrangements of packing, i.e., simple cubic (SC) and body-centred cubic (BCC) has been used for analysis.

All material properties of constituent phases, i.e., fiber and matrix are given in Table 4.1.

Table 4.1 Material properties of fiber and matrix phases

Material Prop.	**$BaTiO_3$ (Fiber)**	**PZT-5H (Matrix)**
C_{11}	166 GPa	126 GPa
C_{12}	77 GPa	55 GPa
C_{13}	78 GPa	53 GPa
C_{33}	162 GPa	117 GPa
C_{44}	43 GPa	35.3 GPa
e_{31}	-4.4 (C/m^2)	-6.5 (C/m^2)
e_{33}	18.6 (C/m^2)	23.3 (C/m^2)
e_{15}	11.6 (C/m^2)	17.0 (C/m^2)
κ_{11}	11.2×10^{-9} (C^2/Nm^2)	15.1×10^{-9} (C^2/Nm^2)
κ_{33}	12.6×10^{-9} (C^2/Nm^2)	13.0×10^{-9} (C^2/Nm^2)

All finite element calculations are made with the finite element package ANSYS 18.0. In analytical as well as in numerical modelling, we assume that the fibers and the constituent are ideally bonded for simplification, and that the fibers are straight and parallel to the x_3-axis. The piezoelectric fibers are uniformly poled along the x_3-direction. Both fiber and matrix are modelled with 20 nodes solid 226, in which strain as well as additional electric potential degree of freedom are used. Firstly, the problem is modelled

as a unit cell (RVE) containing major features of the underlying microstructure. Both the mechanical and physical properties of the constituent material are always considered in micro scale. A finite element mesh is generated from the ANSYS pre-processor and then constraints or boundary conditions are applied to the RVE. The convergence study shows that the meshes have to be fine (approx. 12330 elements) for 0-3 or short-fiber composites. Figure 4.1(b) shows the convergence plot for the selection of mesh size. For the calculation of effective coefficients, we consider a piezoelectric fiber embedded in a piezoelectric matrix. The material parameters of matrix and fiber are listed in Table 4.1, which are chosen for present study. To find the effective coefficients, special load cases with different boundary conditions must be conducted. For a particular load case, only one component value in the strain or electric field vector in Eqn. (4.40b) is non-zero and all others become zero. Then from one row in Eqn. (4.40b), the corresponding coefficient can be calculated via the calculated average values in the stress or electrical displacement vector. Five different volume fractions in the range from 0.1 to 0.5 with the step of 0.1 are calculated in every load case and the representative shapes with two different fiber arrangements; simple cubic (SC) and body centred cubic (BCC) are shown in Figure 4.2 and 4.3. Since the fiber volume fraction has an influence on the results, the size of the unit cell is chosen with unit length in all directions.

4.4.1. Calculation of Effective Properties through FEM

This study has been limited to quasi-static analysis of periodic structures with perfectly bonded fibers, aligned and poled along the axis 3. Figure 4.1(a) illustrates this point in case of a 0-3 composite with a SC and BCC distribution of spheroids. The dimensions of the unit cell are chosen in consonance with the ratio of distance between inclusion centres to satisfy the fibers aspect ratio. Aspect ratio a has been chosen as 1 for both methods, i.e., Eshelby Method and FEM. Due to symmetry, the whole macroscopic

structure is disintegrated into smaller units that contain sufficient information about both fiber and matrix materials known as representative volume elements (RVE). Average results of the properties studied on such RVE provides the overall effective properties at macroscopic level.

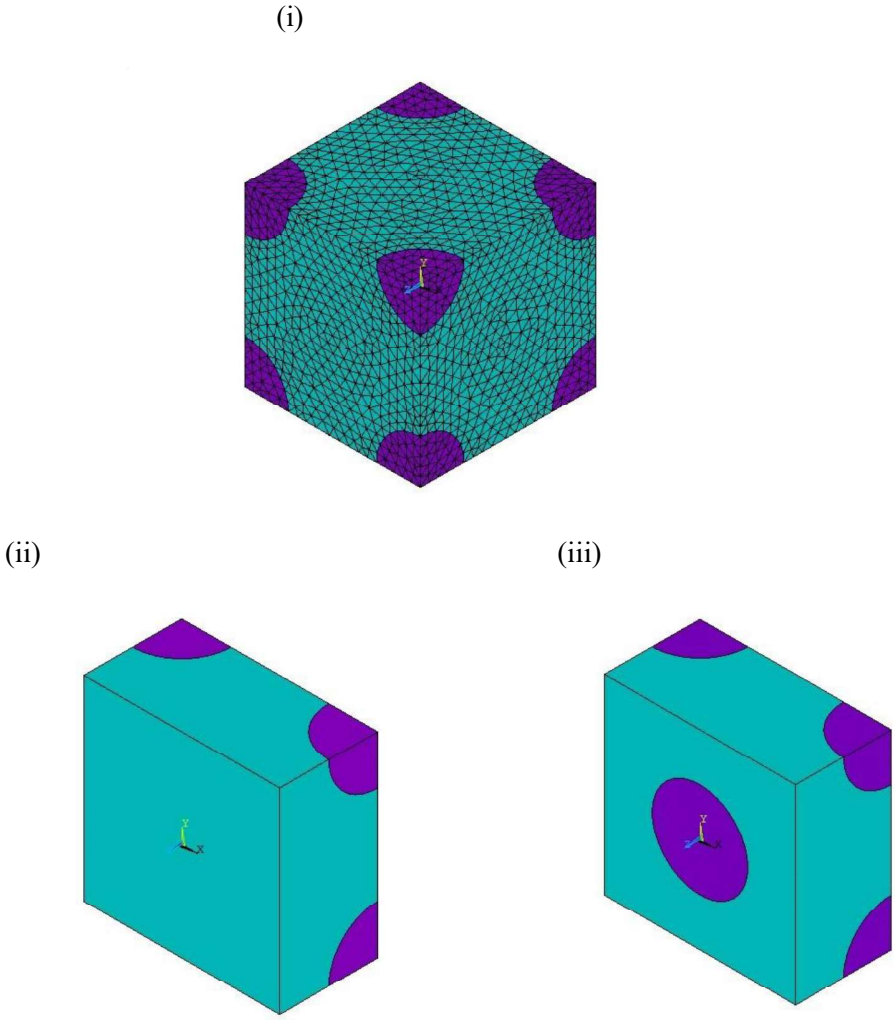

Figure 4.1(a) FEA model of an active composite containing spheroid inclusion; (i) Structure of composite (mesh element view); (ii) RVE of SC fiber arrangement (inner inclusion view); (iii) RVE of BCC fiber arrangement (inner inclusion view).

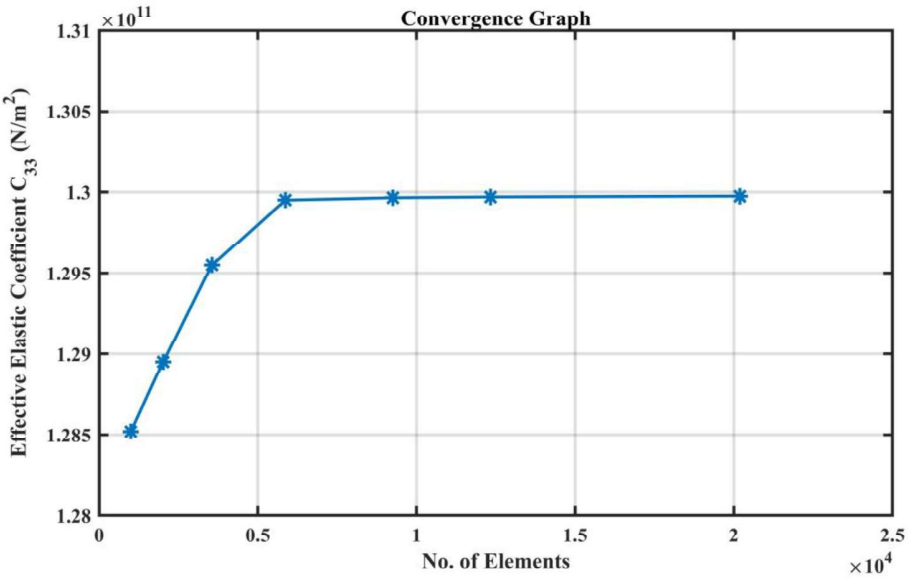

Figure 4.1(b) The convergence graph for determining ideal mesh size for the FE analysis

4.4.2 Boundary Conditions and Parameter Calculations

Constitutive relation given by Eqn. (4.31) suggests that in order to calculate effective elastic coefficients C_{11}^{eff}, C_{12}^{eff}, C_{13}^{eff} and C_{33}^{eff}, all strains and electric field component of the matrix form must be zero except for a non-zero strain produced at surface $x = 1$ for calculating first three coefficients and at surface $z = 1$ for calculating the last one. In order to constrain all other surfaces to remain plane under loading following boundary conditions are imposed.

$$\begin{cases} u_x = 0 & x = 0 \\ u_y = 0 & y = 0 \\ u_z = 0 & z = 0 \end{cases} \tag{4.42}$$

where u_x, u_y and u_z are the displacements along x, y and z directions respectively. Also, the shear stresses on x, y and z planes are set to zero so that these three directions will remain principal directions of stresses. In order to stop charge transfer between opposite

surfaces, the potential degree of freedom is set to zero. From the first and third row of the constitutive Eqn. (4.41) effective coefficients can be obtained.

When $E_i = 0$ $(i = 1,2,3)$, $S_{22} = S_{33} = 0$ and $S_{11} \neq 0$, then following matrix relation shown in Eqn. (4.41)

$$C_{11}^{eff} = \frac{\langle T_{11} \rangle}{\langle S_{11} \rangle}, \qquad C_{12}^{eff} = \frac{\langle T_{22} \rangle}{\langle S_{11} \rangle}, \qquad C_{11}^{eff} = \frac{\langle T_{33} \rangle}{\langle S_{11} \rangle}, \tag{4.43}$$

And, when $E_i = 0$ $(i = 1,2,3)$, $S_{11} = S_{22} = 0$ and $S_{33} \neq 0$,

$$C_{33}^{eff} = \frac{\langle T_{33} \rangle}{\langle S_{33} \rangle}. \tag{4.44}$$

In order to calculate C_{44}^{eff} and C_{66}^{eff} and in-plane shear strain S_{23} must have a non-zero value in strain vector in Eqn. (4.41) and out-of-plane shear strain S_{12} must have a non-zero value. Normal strains on all six faces remain zero and a zero electric field is applied to all surfaces. Now, the fourth and sixth row of constitutive relation will give effective coefficients C_{44}^{eff} and C_{66}^{eff}. Numerically, this can be shown as

When $E_i = 0$ $(i = 1, 2, 3)$, $S_{ii} = 0$ $(i = 1, 2, 3)$, and $S_{23} \neq 0$ or $S_{31} \neq 0$ then,

$$C_{44}^{eff} = \frac{\langle T_{23} \rangle}{\langle S_{23} \rangle} \quad \text{or} \quad C_{44}^{eff} = \frac{\langle T_{31} \rangle}{\langle S_{31} \rangle} \tag{4.45}$$

And, when $E_i = 0$ $(i = 1, 2, 3)$, $S_{ii} = 0$ $(i = 1, 2, 3)$, and $S_{12} \neq 0$,

$$C_{66}^{eff} = \frac{\langle T_{12} \rangle}{\langle S_{12} \rangle} \tag{4.46}$$

$\langle T_{ij} \rangle$ and $\langle S_{kl} \rangle$ are average elemental values of stresses and strains in $x, y, and\ z$ directions.

Similarly, other effective coefficients could also be calculated by altering boundary conditions. The effective piezoelectric constants e_{31}^{eff}, e_{33}^{eff} and the effective dielectric

constant κ_{33}^{eff} are calculated by setting a non-zero electric potential at $z = 1$. The electric potential at all other surfaces will remain zero. Normal strains at all faces will also be constrained. Now, according to the constitutive Eqn. (4.41), the ninth row gives the following solution.

When $S_{ii} = 0\ (i = 1, 2, 3)$, and $E_3 \neq 0$,

$$e_{31}^{eff} = \frac{\langle T_{11} \rangle}{\langle E_3 \rangle}, \quad e_{33}^{eff} = \frac{\langle T_{33} \rangle}{\langle E_3 \rangle} \quad \text{and} \quad \kappa_{33}^{eff} = \frac{\langle D_3 \rangle}{\langle E_3 \rangle} \tag{4.47}$$

$\langle E_3 \rangle$ and $\langle D_3 \rangle$ are average elemental values of electric field and dielectric constants in z-direction. Other remaining coefficients e_{15}^{eff} and κ_{11}^{eff} can be calculated from the seventh row of the matrix relation shown by constitutive Eqn. (4.41) and altering few boundary conditions. For calculating effective piezoelectric constant e_{15}^{eff}, a non-zero value is given to in-plane shear S_{31} and rest other strains and electric field vectors are set as zero. While, the effective dielectric constant κ_{11}^{eff} is obtained by putting a non-zero electric potential at $x = 1$ surface, rest other strains and electric field remains zero.

When $E_i = 0\ (i = 1, 2, 3)$, $S_{ii} = 0\ (i = 1, 2, 3)$, and $S_{31} \neq 0$,

$$e_{15}^{eff} = \frac{\langle D_1 \rangle}{\langle S_{31} \rangle}. \tag{4.48}$$

And, when $S_{ii} = 0\ (i = 1, 2, 3)$, and $E_1 \neq 0$, then,

$$\kappa_{33}^{eff} = \frac{\langle D_1 \rangle}{\langle E_1 \rangle} \tag{4.49}$$

$\langle E_1 \rangle$ and $\langle D_1 \rangle$ are average elemental values of electric field and dielectric constants in x-direction. All the average elemental values can be obtained from ANSYS Post Processing. Figure 4.2 and 4.3 shows a representation of fields within an RVE in an FE analysis for SC and BCC fiber arrangements, respectively.

(a) (b)

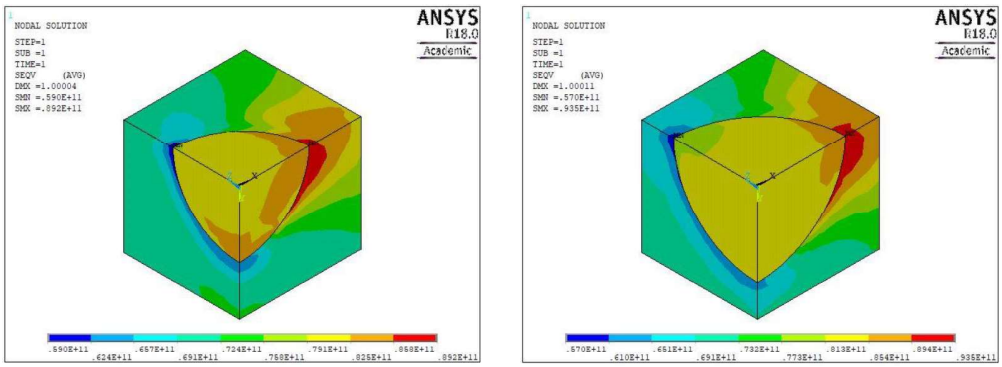

(c) (d)

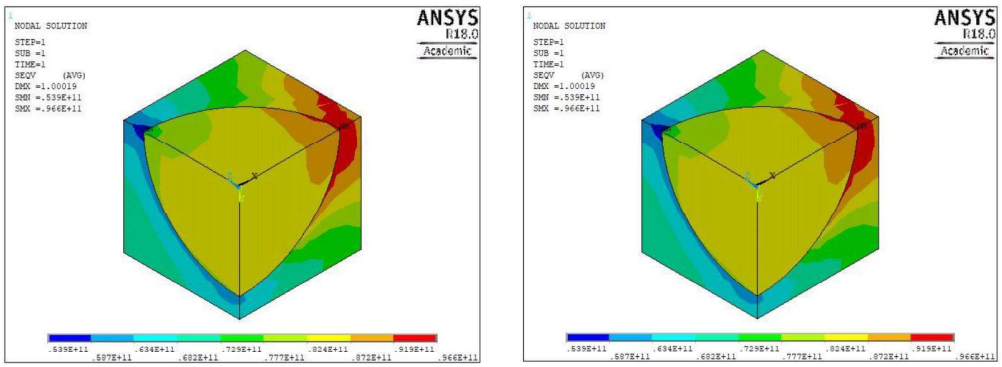

(e)

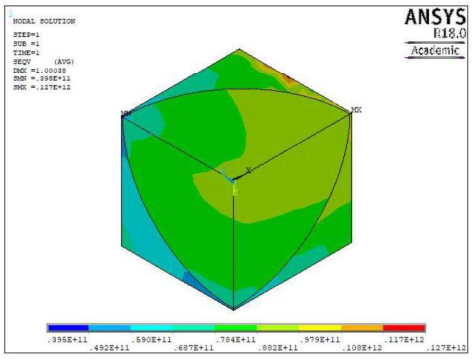

Figure 4.2 Representative Volume Element (RVE) depicting von Mises stress distribution containing spheroid inclusion in SC arrangement (Fiber volume fraction ranging from 0.1-0.5), (a) 0.1, (b) 0.2, (c) 0.3, (d) 0.4, (e) 0.5.

(a) (b)

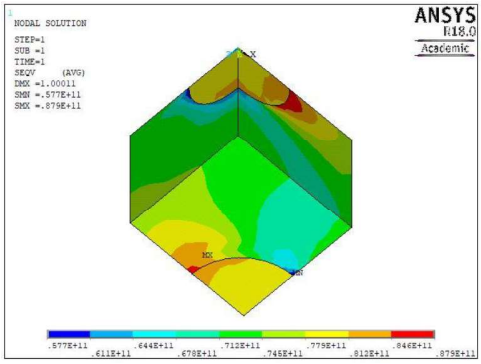

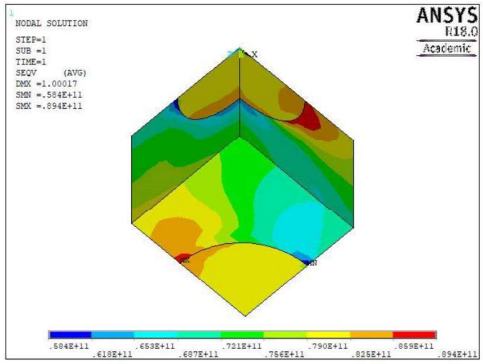

(c) (d)

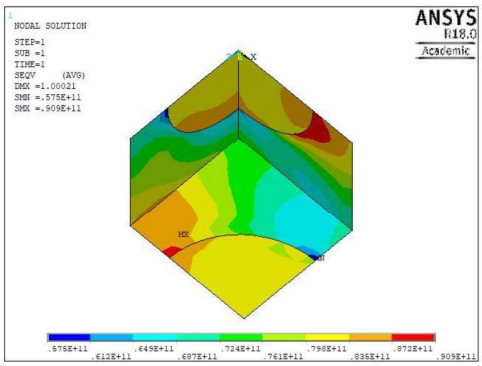

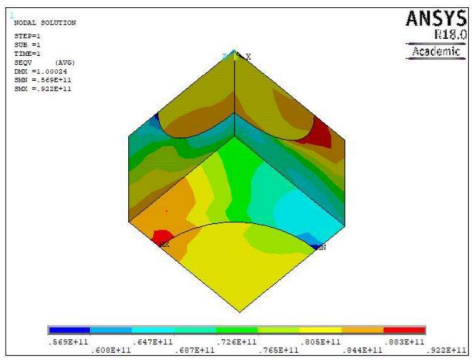

(e)

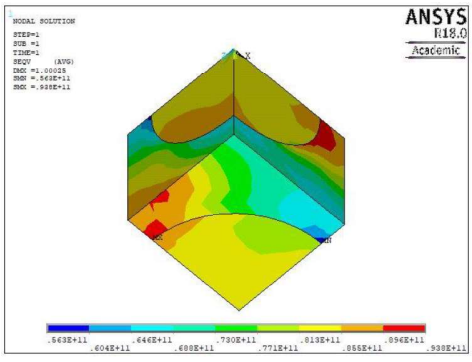

Figure 4.3 Representative Volume Element (RVE) depicting von Mises stress distribution containing spheroid inclusion in BCC arrangement (Fiber volume fraction ranging from 0.1-0.5), (a) 0.1, (b) 0.2, (c) 0.3, (d) 0.4, (e) 0.5.

4.5 Results and Discussion

The finite element method is applied to calculate properties of piezoelectric particulate composite fiber spheroid in shape. All eleven effective coefficients have been calculated for five discrete fiber volume fractions and the results show in general a good coincidence between calculations, via. Eshelby Tensor method and Finite Element Method. Considering the piezoelectric composite as active-active fiber matrix composite in this paper, the predictions of the effective elastic, piezoelectric and dielectric coefficients are compared to the results of the analytical results obtained by Eshelby Method. Figure 4.4-4.9 show the comparison of elastic coefficients, while Figure 4.10-4.14 show the comparison for piezoelectric and dielectric coefficients.

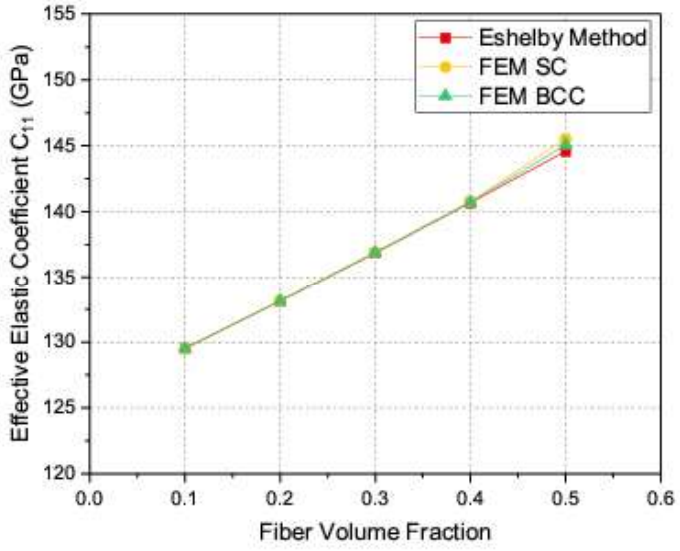

Figure 4.4 Comparison of the predicted effective elastic coefficient C_{11} of BaTiO3/PZT-5H composite with respect to fiber volume fraction.

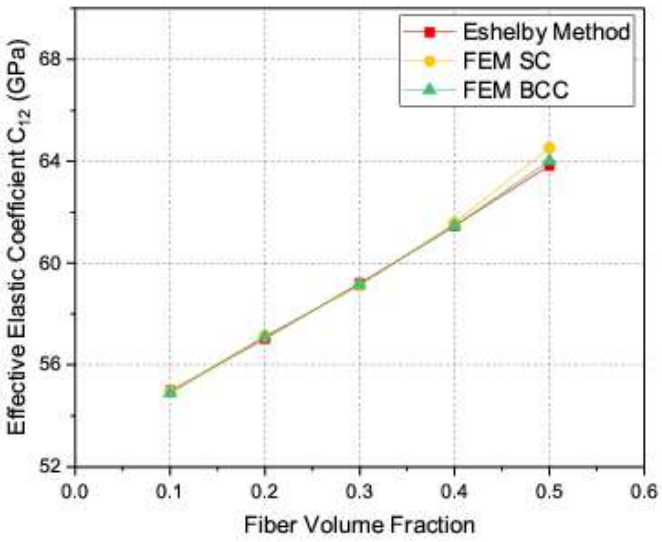

Figure 4.5 Comparison of the predicted effective elastic coefficient C_{12} of BaTiO3/PZT-5H composite with respect to fiber volume fraction.

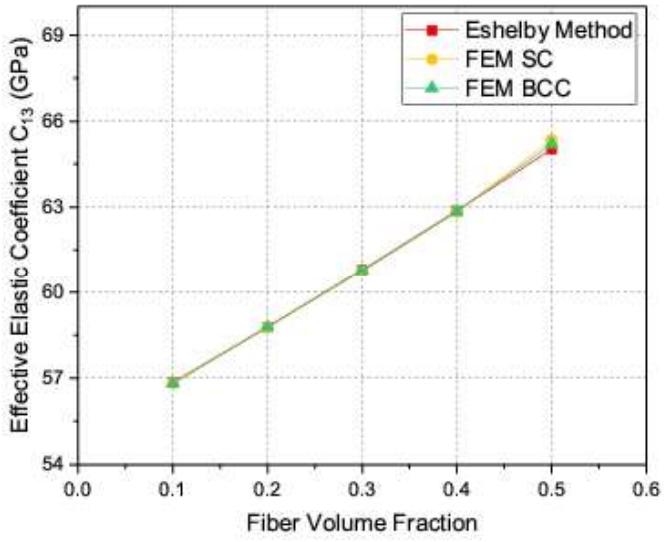

Figure 4.6 Comparison of the predicted effective elastic coefficient C_{13} of BaTiO3/PZT-5H composite with respect to fiber volume fraction.

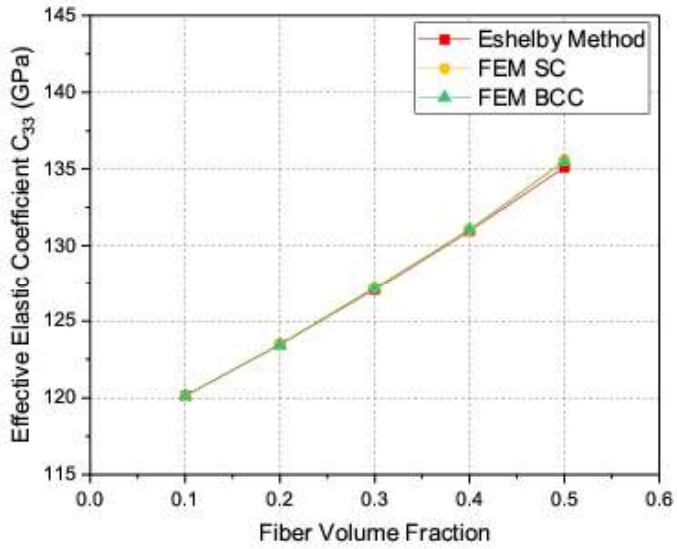

Figure 4.7 Comparison of the predicted effective elastic coefficient C_{33} of BaTiO3/PZT-5H composite with respect to fiber volume fraction.

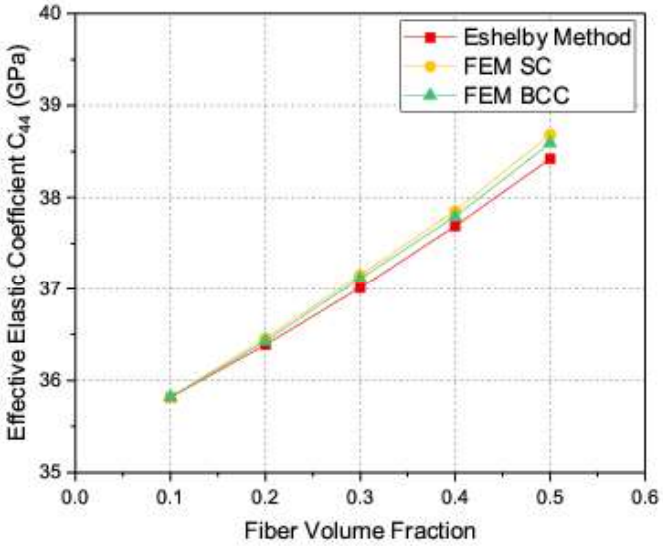

Figure 4.8 Comparison of the predicted effective elastic coefficient C_{44} of BaTiO3/PZT-5H composite with respect to fiber volume fraction.

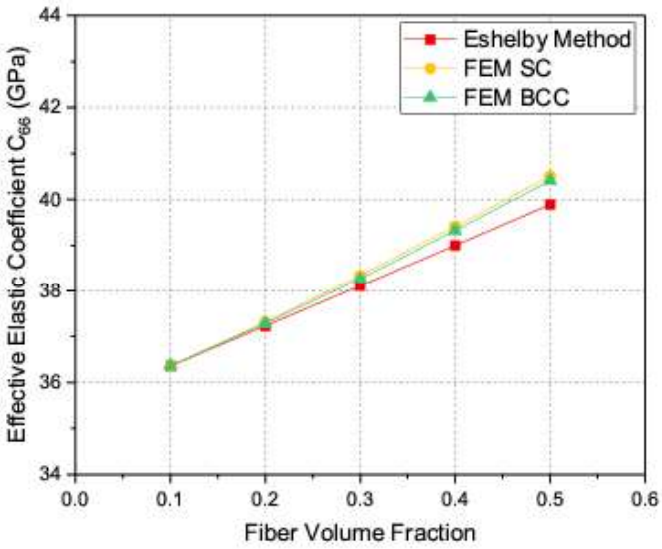

Figure 4.9 Comparison of the predicted effective elastic coefficient C_{66} of BaTiO3/PZT-5H composite with respect to fiber volume fraction.

These figures show that the coefficients C_{11}, C_{33}, e_{33}, and κ_{33} calculated by FEM are in a very good agreement with those obtained by Eshelby Method in all ranges of volume fractions. Quantitatively, the behaviour of the coefficients C_{12}, C_{13}, e_{31}, and κ_{11} is same, although for the greater value of the volume fraction ($v_f = 0.4$ or higher), the curves are not so close. The deviation in results at higher fiber volume fraction ($v_f = 0.4$ or higher) between FEM results and Eshelby Method may be attributed to the fact that the SC and BCC arrangements of fibers does not strictly fulfil the assumptions of transverse isotropy in the Eshelby Method results.

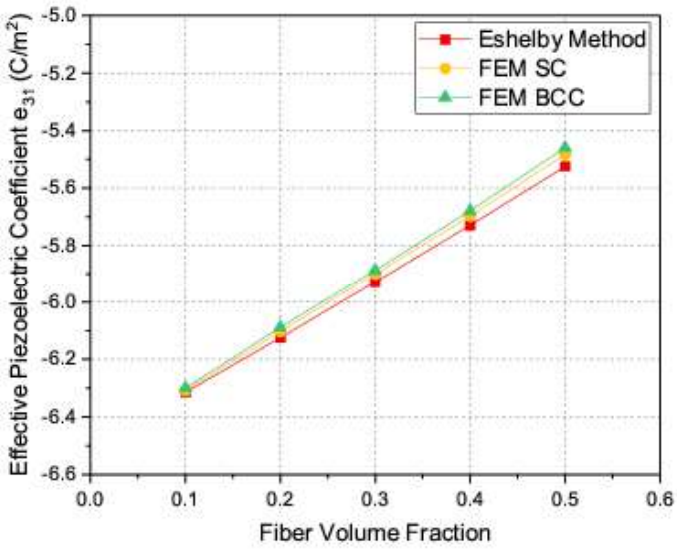

Figure 4.10 Comparison of the predicted effective piezoelectric coefficient e_{31} of BaTiO3/PZT-5H composite with respect to fiber volume fraction.

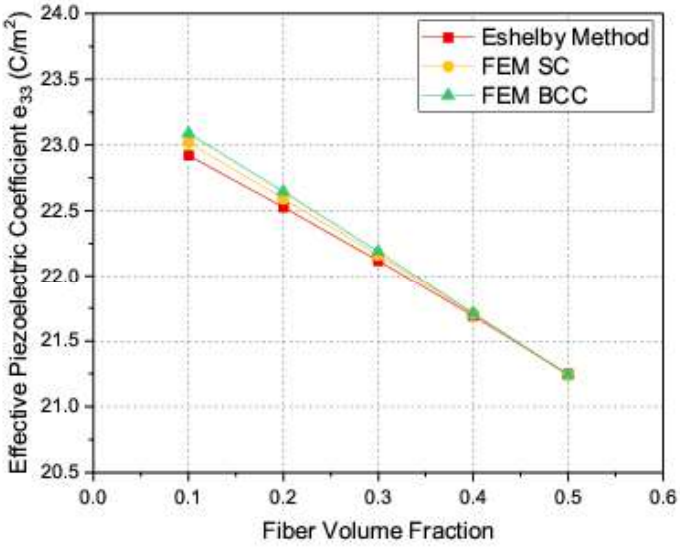

Figure 4.11 Comparison of the predicted effective piezoelectric coefficient e_{33} of BaTiO3/PZT-5H composite with respect to fiber volume fraction.

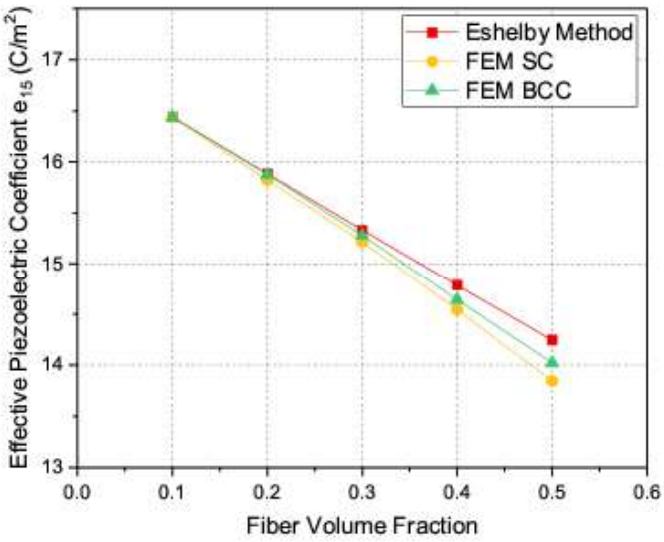

Figure 4.12 Comparison of the predicted effective piezoelectric coefficient e_{15} of BaTiO3/PZT-5H composite with respect to fiber volume fraction for the analytical Eshelby Method and numerical FEM Method.

The results of FEM BCC arrangement of fibers are closer to the results of Eshelby Method, that is because of better capture of interaction between elastic and electric fields of multiple inclusions. The behaviour of coefficients C_{44}, C_{66} and e_{15} obtained from FEM is most divergent in all throughout the range of fiber volume fraction. This must be attributed to the fact that in FEM these results have been obtained by putting in-plane and out-plane shear forces as boundary conditions but it's not so in Eshelby Method as it is approximated based on far-field approach at finite concentrations of inclusions, i.e., Mori-Tanaka mean field theory.

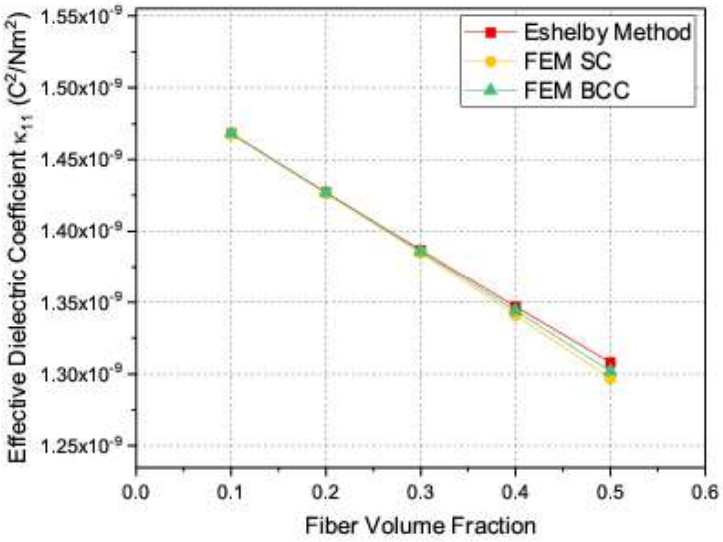

Figure 4.13 Comparison of the predicted effective dielectric coefficient κ_{11} of BaTiO3/PZT-5H composite with respect to fiber volume fraction.

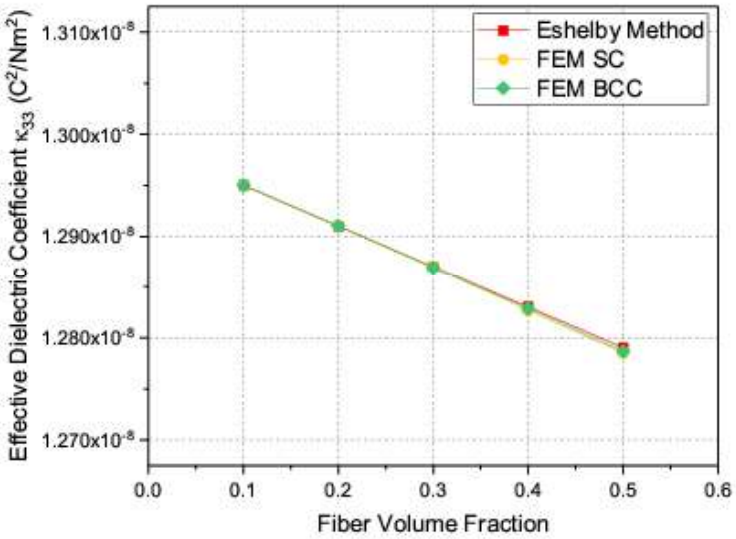

Figure 4.14 Comparison of the predicted effective dielectric coefficient κ_{33} of BaTiO3/PZT-5H composite with respect to fiber volume fraction.

Moreover, it is observed that finite element method results in case where boundary condition is set as longitudinal plane stress, shows a large degree of agreement with Eshelby Method results throughout the given range of fiber volume fraction while when shear stresses are set as a boundary condition the finite element method result shows a larger diversion from the result obtained by Eshelby Method. FEA only provides a best approximation to the possible solution but the Eshelby model is based on the exact solutions of electroelastic Eshelby tensors. Moreover, doing FEA over discrete fibre volume fractions (0.1-0.6 with a step of 0.1) involves repeated procedures that proves to be time consuming and uneconomical. The Eshelby model provides the exact results and by using these results the properties can be characterized for the whole range of fiber volume fractions (0.0-1.0).

4.6 Summary

A numerical approach is adopted to evaluate the effective coefficients of piezoelectric particulate composite through the Eshelby Method. Later, a finite element approach is adopted using FE package ANSYS 18.0 to evaluate effective coefficients with two different inclusion arrangements: simple cubic (SC) and body centred cubic (BCC). The results have been compared graphically for all individual coefficients with both these methods. Compared with the results, the technique in the present paper provides reliable results, indicating that this technique can be easily extended for determining homogenized material data for more complex composites. The obtained results also suggest that the effect of shear stress as boundary condition and inclusion-inclusion interaction is better captured in FEM than Eshelby Method. This study also provides an insight that strength of materials SM methods for approximation of effective properties only holds good in case of long fiber composite. In the short fiber case, its

prediction of properties is far from accurate, so it can't be used in studying the effective properties of particulate composite.

Though this study carries a geometric shape of fiber as spherical particulate and two arrangements of particles as SC and BCC in finite element modelling, study based on other shapes and configuration can also be carried out to obtain more generalized results. Since rule of mixture is a reliable form of study especially in case of long continuous fiber problem but this predicts a very poor approximation of effective properties in case of randomly oriented discontinuous fiber therefore in such scenario Eshelby model map the problem quite effectively and prediction of properties using averaging method given by Mori- Tanaka gives a close approximation of effective properties. The results of finite element study also suggest the same as much of the coefficients shows quite similar behaviour for the range of fiber volume fraction of the study.